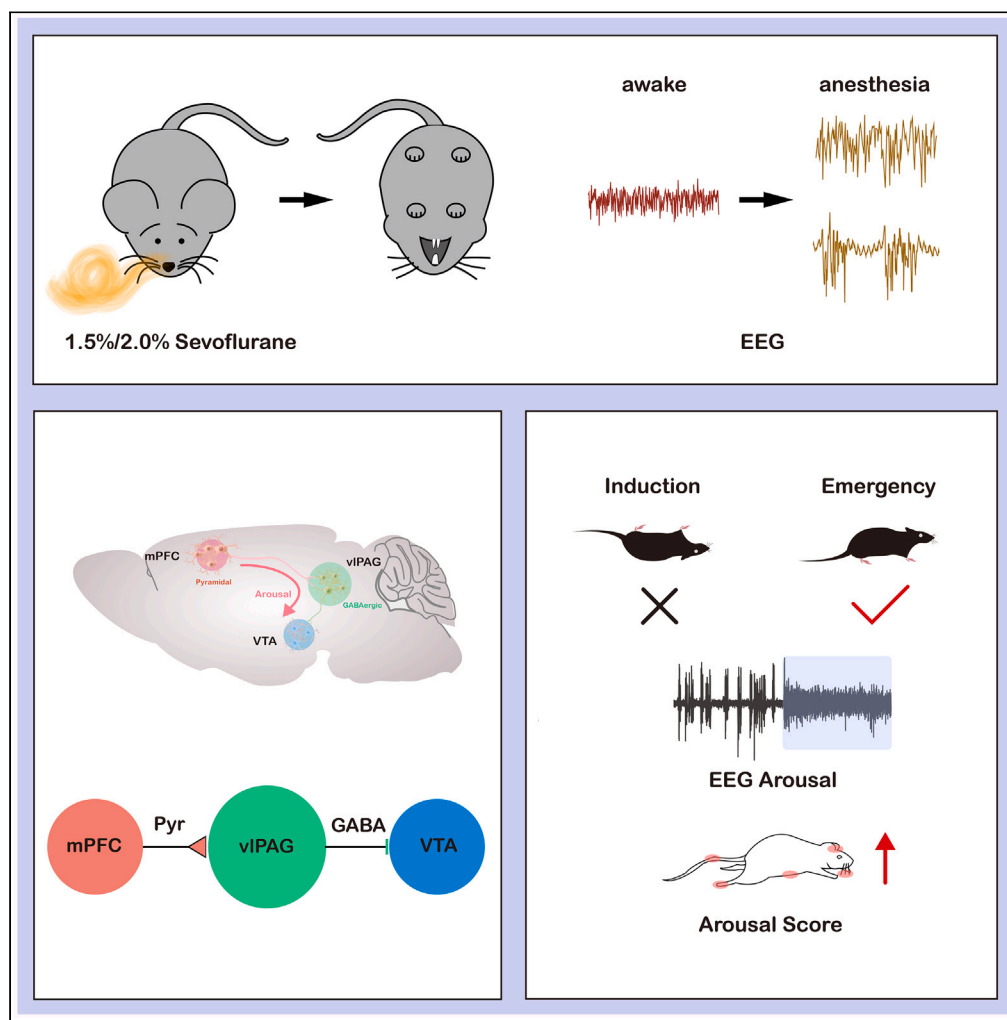## Article

Ventrolateral periaqueductal gray GABAergic neurons promote arousal of sevoflurane anesthesia through cortico-midbrain circuit

Yongxin Guo,
Yanping Song,
Fuyang Cao, ...,
Yanhong Liu,
Weidong Mi, Li
Tong

mmwwd1962@163.com (W.M.)
tongli301@aliyun.com (L.T.)

Highlights

VlPAG^{GABA} neuronal
dynamics reflect awake
state during sevoflurane
anesthesia

Activating vlPAG^{GABA}
neurons promote arousal
after sevoflurane
anesthesia

VlPAG^{GABA} neurons
modulate emergence
from anesthesia via mPFC-
vlPAG-VTA circuit

Article

Ventrolateral periaqueductal gray GABAergic neurons promote arousal of sevoflurane anesthesia through cortico-midbrain circuit

Yongxin Guo,[1,4] Yanping Song,[2,4] Fuyang Cao,[3,4] Ao Li,[1] Xinyu Hao,[1] Wenzhu Shi,[1] Zhikang Zhou,[1] Jiangbei Cao,[1] Yanhong Liu,[1] Weidong Mi,[1,*] and Li Tong[1,5,*]

SUMMARY

The mechanism of general anesthesia remains elusive. The ventrolateral periaqueductal gray (vlPAG) in the midbrain regulates sleep and awake states. However, the role of vlPAG and its circuits in anesthesia is unclear. We utilized opto/chemogenetics, righting reflex, and electroencephalographic recording to assess consciousness changes. We employed fiber photometry to measure the activity of neurons and neurotransmitters. As a result, photometry recording showed that the activity of GABA neurons in vlPAG decreased during sevoflurane anesthesia and was reactivated after anesthesia. Activating GABAergic neurons in vlPAG promoted arousal during anesthesia, while inhibiting them delayed this process. Furthermore, medial prefrontal cortex (mPFC) to vlPAG pyramidal neurons projections and vlPAG to ventral tegmental area (VTA) GABAergic projections played a prominent role in the anesthesia-awake transition. GABA neurotransmitter activity of VTA synchronized with mPFC-vlPAG pyramidal neuron projections. Therefore, the cortico-midbrain circuits centered on vlPAG GABAergic neurons exert an arousal-promoting effect during sevoflurane anesthesia.

INTRODUCTION

The mechanism underlying general anesthesia remains an enigma in the field of neuroscience. The involvement of excitatory and inhibitory neurotransmitters in the regulation of general anesthesia during the loss and recovery of consciousness induced by general anesthetics is still unclear.[1]

Several neural areas, such as the cortex, thalamus, hypothalamus, and midbrain, are involved in regulating the mechanisms of general anesthesia.[2–5] The midbrain is considered a putative site for the origin of some forms of consciousness in vertebrates.[6,7] Many studies have suggested that the midbrain dopaminergic and serotoninergic systems are involved in regulating anesthetic arousal.[8–10] The midbrain central gray, also known as the periaqueductal gray (PAG), is a structure that surrounds the cerebral aqueduct.[11,12] It plays an essential role in regulating pain, autonomic nervous system, defense response, depressive behavior, and sleep.[13–15]

Gamma-aminobutyric acid (GABAergic) neurons in the ventrolateral periaqueductal gray (vlPAG) are known to be important for regulating sleep state transitions.[15] But the role of vlPAG[GABA] neurons in the regulation of sevoflurane anesthesia remains unclear.

Synchronization of thalamic-cortical circuits and subcortical ascending activation system (Bottom-Up) play essential roles in the regulation of anesthesia.[16–18] Gradually increasing evidence points to the 'top-down' regulatory model may play an equally important role in anesthesia-wake regulation.[19,20] But the mechanism of the descending pathway in the cortical-midbrain in general anesthesia remains elusive.

The vlPAG receives projections from the cortex,[21] and mPFC-vlPAG projection is involved in aversive and compulsive behavioral responses, as well as pain modulation.[22,23] This study hypothesized that vlPAG[GABA] neurons promote arousal from anesthesia through the cortico-midbrain (Top-Down) model in mice.

RESULTS

Neuronal activity of vlPAG^{GABA} neurons was inhibited during sevoflurane anesthesia and activated in the awake state

To directly investigate the activity of vlPAG^{GABA} neurons during anesthesia-wake states, we utilized fiber photometry to detect calcium signals in these neurons. We injected *AAV2/9-GAD67-GCaMP6s* (120 nL, titter: 3.54 ×10^{12} v.g./mL, unilaterally) into male mice to induce the expression of calcium indicators in GABAergic neurons. Immunofluorescence staining confirmed the positive expression of GABA in GCaMP6s-expressing cells (Figure 1C). Our results showed that vlPAG GABAergic neuronal activity was inhibited during 2.0% sevoflurane anesthesia, as indicated by a gradual decrease in calcium activity (Pre vs. Post: −0.40 ± 0.50% vs.-14.8 ± 2.95%, p = 0.0013, n = 5 vs. 5) (Figures 1D and 1E). The calcium activity gradually recovered after the cessation of anesthetic inhalation (Pre vs. Post: 1.19 ± 0.72% vs.−28.61 ± 4.97%, p = 0.0003, n = 5 vs. 5) (Figures 1F and 1G). Collectively, Neuronal activity of vlPAG^{GABA} neurons was inhibited during sevoflurane anesthesia and activated in the awake state.

Additionally, we observed changes in EEG signals that correlated with the elevation of calcium signals during 2.0% sevoflurane inhalation. The waveform of the EEG signals changed from an anesthetic wave to an arousal-like wave (Figure 1H), and the spectrum analysis of EEG showed decreased delta power (45.5% ± 5.7% vs. 30.5% ± 3.1%, p = 0.049) and increased power in beta (9.6% ± 1.6% vs. 14.0% ± 1.0%, p = 0.045) and gamma (15.7% ± 0.8% vs. 23.5% ± 1.6%, p = 0.0019) bands with the elevation of calcium signal (Figure 1I).

Optical activation vlPAG^{GABA} neurons promotes arousal from sevoflurane anesthesia

To investigate the role of vlPAG^{GABA} neurons in sevoflurane anesthesia regulation, we utilized the *AAV2/9-GAD67-ChR2-GFP* (100 nL, titter: 5.10×10^{12} v.g./mL, unilaterally) virus to transfect light-sensitive channelrhodopsin-2 protein (ChR2) to activate neurons (Figure 2A). Photostimulation (5-10 mW, 20 Hz, 10 ms duration, 1s-on/1s-off cycle) was performed simultaneously with the onset of sevoflurane and ended until loss of righting reflex (LORR), which did not affect anesthesia induction time (ChR2-vs. ChR2+: 191.7 ± 11.9s vs. 209.2 ± 10.44s, p = 0.2944, n = 6 vs. 6). Photostimulation was performed simultaneously with the cessation of sevoflurane and ended until recovery of righting reflex (RORR), and it was found that optical activation of the GABAergic neurons shortens the arousal time (ChR2-vs. ChR2+: 240.0 ± 18.6s vs. 134.0 ± 11.40s, p = 0.0045, n = 6 vs. 6) (Figure 2C). Additionally, optical stimulation was performed for 2 min during 2.0% sevoflurane anesthesia maintenance, and the changes in EEG during anesthesia were observed (Figure 2E). EEG burst suppression ratio (BSR) during 2.0% sevoflurane maintenance decreased upon optical stimulation (ChR2-vs. ChR2+ in 4th min: 50.1 ± 6.1% vs. 17.5 ± 7.0%, p = 0.0141, n = 6 vs. 6) (Figure 2G).

We administered 1.5% sevoflurane to investigate whether stimulation of vlPAG^{GABA} neurons could induce emergence behaviors under light anesthesia (Figure 2F). At 20–22 min of light stimulation (Figure 2H), the percentages of power in the delta band reduced obviously (F [2, 15] = 16.23, p = 0.0002), while those in the alpha (F [2, 15] = 4.022, p = 0.04), beta (F [2, 15] = 20.70, p < 0.0001) and the gamma (F [2, 15] = 12.65, p = 0.0006) bands significantly increased in ChR2+ group (Figure 2I). Furthermore, a notable increase in behavioral arousal scores was observed (ChR2-vs. ChR2+: p = 0.0022, n = 6 vs. 6) (Figure 2J). There was no change in the EEG power spectra of the ChR2-animals after stimulation. The promoting-arousal effect of vlPAG GABAergic neurons was further confirmed using Vgat-Cre mice (Figure S2).

Therefore, optical activation vlPAG^{GABA} neurons could induce the awakening of anesthesia maintenance and promote the recovery of sevoflurane anesthesia.

Chemogenetic regulation of vlPAG^{GABA} neurons modulates arousal during sevoflurane anesthesia

To confirm the continuous effects of vlPAG^{GABA} neurons under general anesthesia, we utilized chemogenetics by injecting *rAAV2/9-GAD67-hM4Di-mCherry* (150 nL, titter: 2.85×10^{12} v.g./mL), *AAV2/9-GAD67-hM3Dq-mCherry* (150 nL, titter: 3.45×10^{12} v.g./mL) or *rAAV2/9-GAD67-mCherry* (150 nL, titter: 2.16×10^{12} v.g./mL) viruses bilaterally into the vlPAG to express mCherry in GABAergic neurons (Figure 3B). Intraperitoneal injection of CNO (1 mg/kg) was performed 1 h before the start of 2.0% sevoflurane to activate vlPAG^{GABA} neurons. Although activation of vlPAG^{GABA} neurons had little effect on induction time (hM3Dq-vs. hM3Dq+: 294.2 ± 14.40s vs. 306.7 ± 12.6s, p = 0.5278, n = 6 vs. 6), the emergence
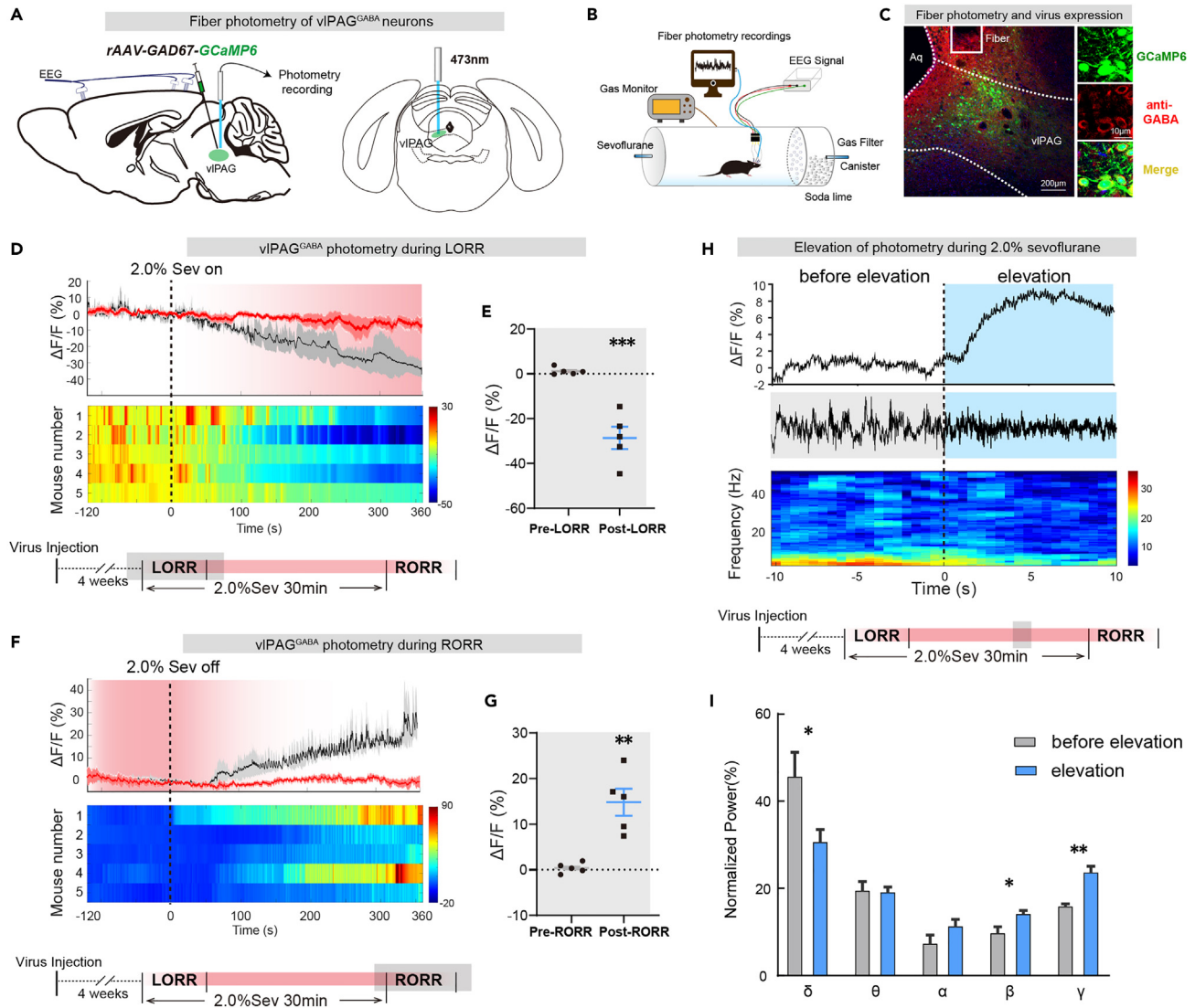
Figure 1. Calcium signal indicates that vlPAG^{GABA} neurons activity is closely related to arousal during sevoflurane anesthesia

(A) Injection of calcium signal viruses into vlPAG schematic.

(B) Schematic of the calcium signal recording configuration.

(C) Representative immunofluorescence showing the calcium signal virus expression and fiber track in vlPAG.

(D) Following the initiation of 2.0% sevoflurane anesthesia, the activity of vlPAG^{GABA} neurons gradually decreased (top), as observed in the heatmaps of neuronal activity changes in five mice (bottom).

(E) The ΔF/F value of vlPAG^{GABA} neurons exhibited a significant decrease after the onset of anesthesia.

(F) After 2.0% sevoflurane anesthesia, the activity of vlPAG^{GABA} neurons gradually increased (top), as demonstrated in the heatmaps of neuronal activity changes in five mice (bottom).

(G) The ΔF/F value of vlPAG^{GABA} neurons increased markedly after anesthesia termination.

(H) Representative elevation changes of calcium signal in vlPAG^{GABA} neurons and corresponding EEG spectrum during anesthesia.

(I) Diagram showing the power percentages in different frequency bands, related to (H). The data is presented as the mean ± SEM, *p < 0.05, **p < 0.01, ***p < 0.001.

time was significantly shortened compared to control groups (hM3Dq-vs. hM3Dq+: 200.8 ± 14.3s vs. 160.0 ± 10.0s, p = 0.0412, n = 6 vs. 6) (Figure 3C).

Moreover, BSR of EEG during 2.0% sevoflurane maintenance was significantly decreased by chemogenetic activation (Figure 3E). The EEG spectrum analysis showed that during the period of 1.5% sevoflurane maintenance, the spectrum produced a decrease in delta power (39.9% ± 1.0% vs. 33.5% ± 0.3%,
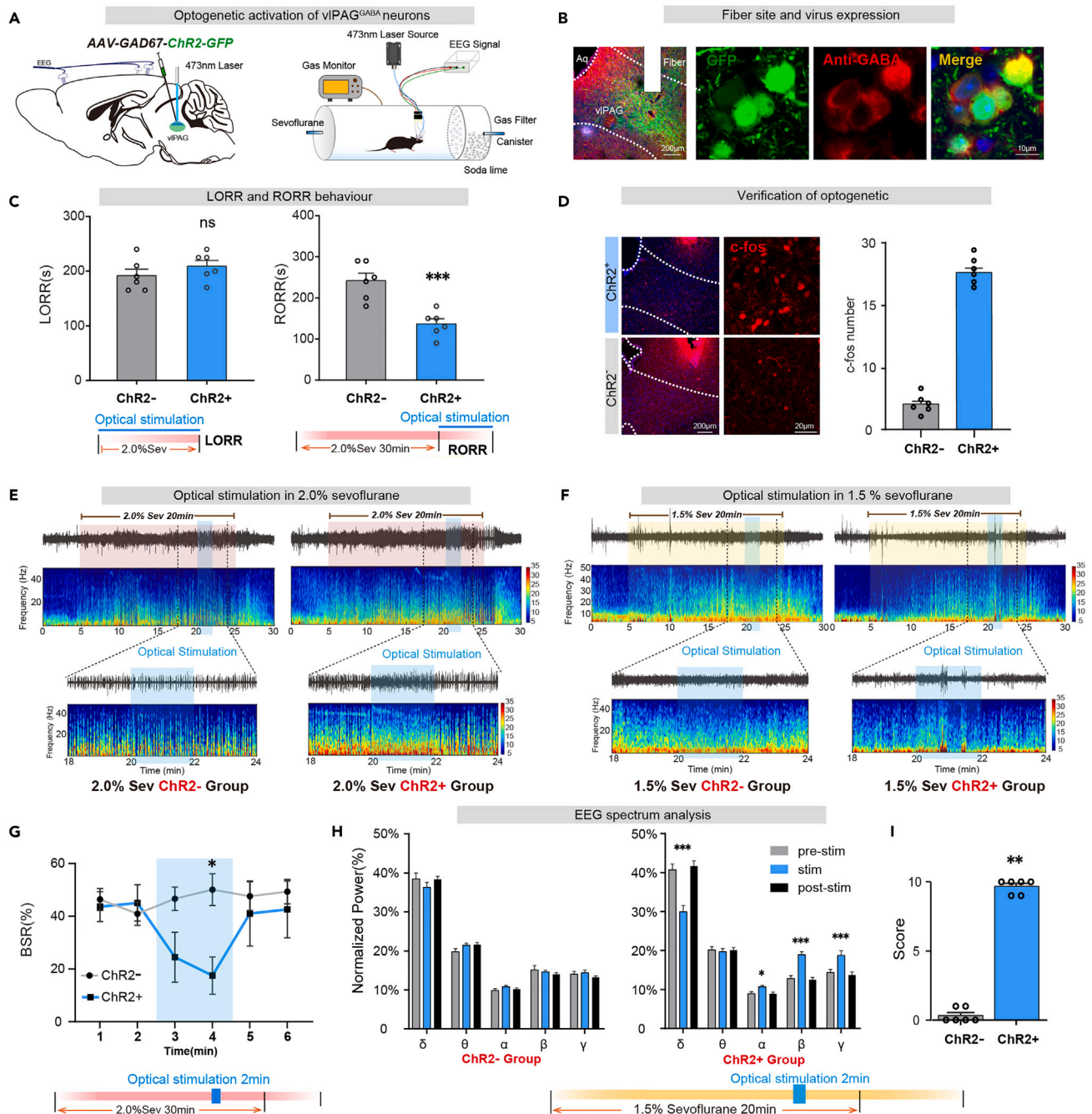
Figure 2. Optical activation of vlPAG^GABA neurons promotes arousal from sevoflurane anesthesia

(A) Schematic diagram of optogenetic virus injection into the vlPAG and laser irradiation(left). Righting reflex detection and EEG recording configuration (right).

(B) The immunofluorescence image shows GFP expression in vlPAG^GABA neurons (red).

(C) Optogenetic activation of vlPAG^GABA significantly shortened RORR time (right).

(D) Immunofluorescence of c-fos (red) in vlPAG. Dramatic increase of c-fos expression in vlPAG activated by optogenetic.

(E) The representative EEG spectrum of the control group (ChR2-group) and the experimental group (ChR2+ group) in 2.0% sevoflurane anesthesia.

(F) The representative EEG spectrum of the ChR2-group and the ChR2+ group in 1.5% sevoflurane anesthesia.

(G) At 20–22 min of light stimulation under 2.0% sevoflurane anesthesia, the ChR2+ group displayed a significantly lower BSR of EEG compared to the ChR2-group.

Figure 2. *Continued*

(H) Compared to the period of 2 min before and after light stimulation, the ChR2+ group exhibited a reduction in the percentage of power within the δ band, and a significant increase in the percentages of power within the α, β, and γ bands under 1.5% anesthesia. There was no difference in the EEG spectrum in the ChR2-group.

(I) During 1.5% sevoflurane anesthesia, at 20–22 min of light stimulation, the ChR2+ group of mice exhibited a significantly higher body movement score than the ChR2-group. The data is presented as the mean ± SEM, *p < 0.05, **p < 0.01, ***p < 0.001.

p = 0.0001), whereas the power in theta (23.2% ± 0.3% vs. 24.9% ± 0.7%, p = 0.0435), beta (12.0% ± 0.5% vs. 14.3% ± 0.6%, p = 0.0110) and gamma (13.7% ± 0.5% vs. 16.3% ± 0.6%, p = 0.0087) bands markedly increased (Figure 3F).

Inhibition of vlPAG^{GABA} neurons prolonged the emergence time (hM4Di-vs. hM4Di+: 179.2 ± 10.7s vs. 229.7 ± 16.3s, p = 0.0267, n = 6 vs. 6), without affecting induction time (hM4Di-vs. hM4Di+: 276.7 ± 9.8s vs. 278.3 ± 28.3s, p = 0.9568, n = 6 vs. 6) (Figure 3G). Furthermore, the hM4Di+ group exhibited elevated BSR of EEG during 2.0% and 1.5% sevoflurane anesthesia compared to the hM4Di-group. [F(10,390) = 23.19, p < 0.001, n = 6 vs. 6] [F(10,390) = 35.16, p < 0.001, n = 6 vs. 6] (Figures 3I and 3J).

Therefore, Long-term regulation of vlPAG^{GABA} neurons can also regulate sevoflurane anesthesia by electroencephalographic and return of righting reflex criteria.

Optical stimulation of vlPAG^{GABA}-VTA projections facilitates arousal from sevoflurane anesthesia

To investigate which downstream nuclei are involved in the regulation of arousal, we injected the *AAV2/9-GAD67-GFP* (100 nL, titter: 6.24×10^{12} v.g./mL, unilaterally) virus to confirm vlPAG^{GABA} neurons projections. Four weeks later, dense viral expression was observed in the VTA, lateral preoptic area (LPO), and zona incerta (ZI), indicating strong vlPAG^{GABA} innervation to these nuclei (Figures 4A and 4B). To clarify the role of vlPAG^{GABA} projections in sevoflurane anesthesia. We injected the *AAV2/9-GAD67-ChR2-GFP* (100 nL, titter: 5.10×10^{12} v.g./mL, unilaterally) virus into the vlPAG and inserted optical fibers into the VTA, LPO, or ZI to stimulate GABAergic terminals (Figures 4C and S1).

Photostimulation of vlPAG^{GABA}-VTA projections facilitated arousal, as evidenced by a shorter time to RORR in the ChR2+ group compared to the control group (ChR2-vs. ChR2+: 200.8 ± 13.6s vs. 149.2 ± 9.2s, p = 0.0102, n = 6 vs. 6) without affecting sevoflurane anesthesia induction (ChR2-vs. ChR2+: 234.2 ± 15.3s vs. 212.5 ± 9.7s, p = 0.2596, n = 6 vs. 6) (Figure 4E). Light stimulation during the maintenance of 2.0% sevoflurane anesthesia also caused changes in the EEG pattern of the ChR2+ group (Figure 4F), with a significant decrease in BSR. (ChR2-vs. ChR2+ at 3rd min: 44.2 ± 2.6% vs. 18.7 ± 5.6%, p = 0.0039, n = 5 vs. 6; ChR2-vs. ChR2+ at 4th min: 42.5 ± 2.3% vs. 25.1 ± 6.3%, p = 0.0395, n = 5 vs. 6) (Figure 4H). Additionally, during 1.5% sevoflurane maintenance, optical stimulation of ChR2+ mice induced a decrease in delta power (F [2, 15] = 22.51, p < 0.0001) and increase in beta (F [2, 15] = 17.50, p = 0.0001) and gamma (F [2, 15] = 36.04, p < 0.0001) bands (Figure 4I). Furthermore, a notable increase in arousal behavioral scores was observed (ChR2-vs. ChR2+: p = 0.0022, n = 6 vs. 6) (Figure 4J). No variance was observed in the EEG power spectra of the ChR2-group.

However, optogenetic activation of GABAergic terminals in the LPO and ZI had no significant effect on sevoflurane anesthesia (Figure S1).

Optical stimulation of mPFC^{Pyr}-vlPAG projections facilitates arousal from sevoflurane anesthesia

Retrograde tracing of vlPAG by *pAAV2/Retro-hSyn-mCherry* (80 nL, titer: 1.12×10^{13} v.g./mL, unilaterally) virus revealed that the upstream of the nucleus was mainly concentrated in the cortex and other regions, particularly in the mPFC. (Figures 5A and 5B). To clarify the role of mPFC^{Pyr}-vlPAG projections in sevoflurane anesthesia, we injected *rAAV2/9-CamKII-ChR2-mCherry* (120 nL, titter: 3.49×10^{12} v.g./mL, unilaterally) or *rAAV2/9-CamKII-mCherry* (100 nL, titter: 3.65×10^{12} v.g./mL, unilaterally) into the mPFC and inserted optical fibers into the vlPAG (Figures 5C and 5D). Four weeks later, c-fos staining results showed that c-fos positive neurons increased in the ChR2+ group (Figure 5G).

Photostimulation of mPFC^{Pyr}-vlPAG projections shortened the emergence time after sevoflurane anesthesia in the ChR2+ group compared to the control group (ChR2-vs. ChR2+: 245.0 ± 18.0s vs. 174.2 ± 7.7s,
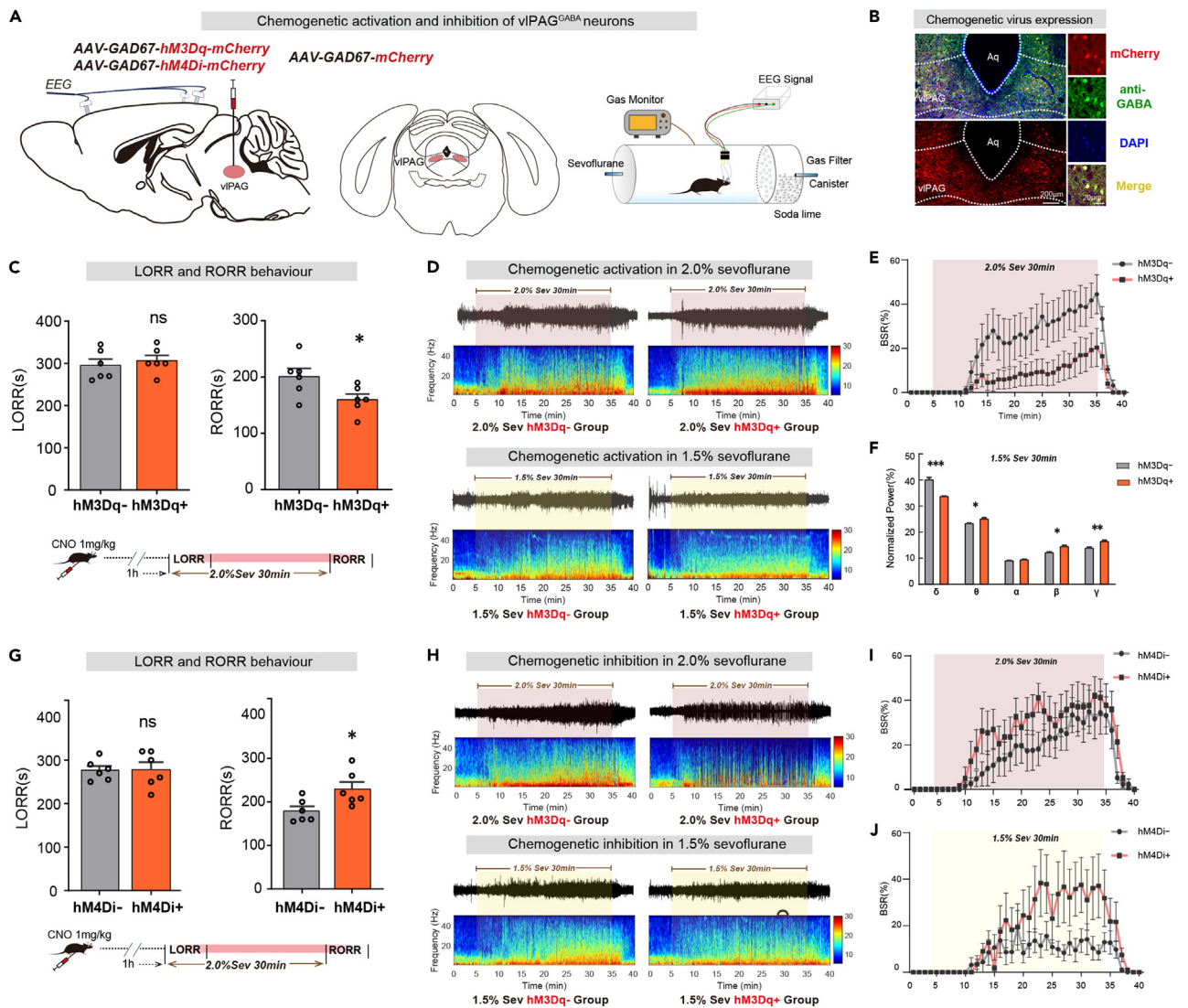
Figure 3. Chemogenetic regulation of vlPAG^GABA neurons modulates arousal during sevoflurane anesthesia

(A) Injection of chemogenetic viruses into vlPAG and EEG recording configuration.

(B) The images show GABAergic neurons (green) expressing chemogenetic virus (mCherry, red).

(C) Activation of vlPAG^GABA significantly shortened RORR time but did not change LORR.

(D) The representative EEG spectrum of the control group (hM3Dq-group) and the experimental group (hM3Dq+ group) in 2.0% (top) and 1.5% (down) sevoflurane anesthesia.

(E) Under 2.0% sevoflurane anesthesia, the hM3Dq+ group exhibited a significantly lower BSR of EEG compared to the hM3Dq-group.

(F) Power spectral analysis of EEG signals shows that the percentage of power in the δ band decreased significantly. In contrast, that in the γ band increased in the hM3Dq+ group more than in the hM3Dq-group during 1.5% sevoflurane anesthesia.

(G) Inhibition of vlPAG^GABA significantly prolonged RORR time but had no significant effect on LORR time.

(H) The representative EEG spectrum of the control group (hM4Di-group) and the experimental group (hM4Di+ group) in 2.0% (top) and 1.5% (down) sevoflurane anesthesia.

(I) Under 2.0% sevoflurane anesthesia, the hM4Di+ group demonstrated a significantly higher BSR of EEG compared to the hM4Di-group.

(J) Under 1.5% sevoflurane anesthesia, the hM4Di+ group displayed a significantly higher BSR of EEG than the hM4Di-group. The data is presented as the mean ± SEM, *$p < 0.05$, **$p < 0.01$, ***$p < 0.001$.

$p = 0.0047$, $n = 6$ vs. 6), without affecting sevoflurane anesthesia induction (ChR2-vs. ChR2+: 216.7 ± 14.1s vs. 202.5 ± 11.7s, $p = 0.4573$, $n = 6$ vs. 6) (Figure 5F). Additionally, BSR of EEG during 2.0% sevoflurane maintenance significantly decreased upon optical stimulation (ChR2-vs. ChR2+ in 3rd min: $28.0 \pm 5.1\%$ vs. $12.7 \pm 4.6\%$, $p = 0.0497$, $n = 6$ vs. 6; ChR2-vs. ChR2+ in 4th min: $29.5 \pm 3.8\%$ vs. $10.0 \pm 4.0\%$, $p = 0.0068$, $n = 6$ vs. 6) (Figure 5J).
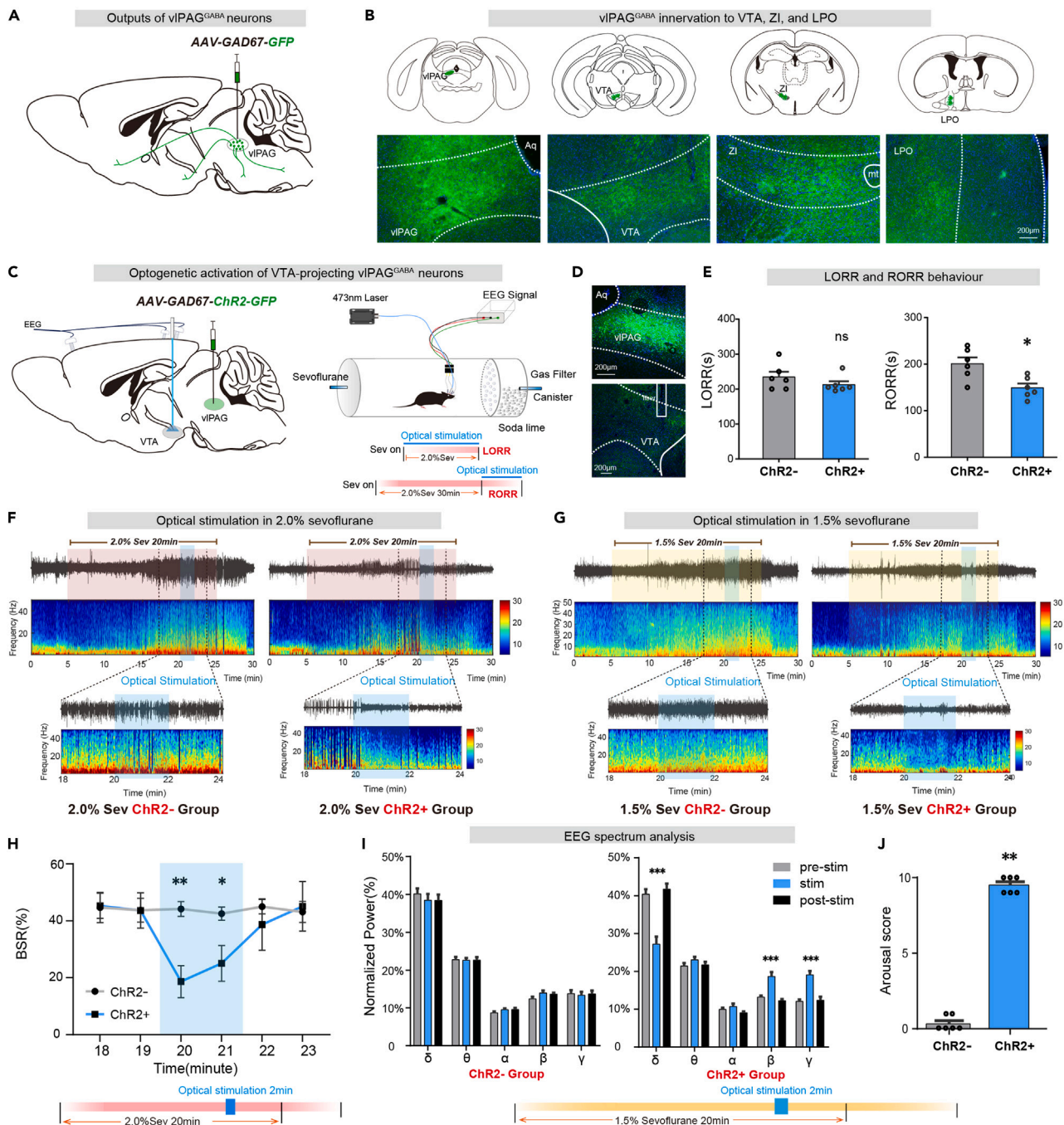
Figure 4. Optical stimulation of vlPAG^GABA-VTA projections facilitates arousal from sevoflurane anesthesia

(A) Anterograde tracing virus injection into vlPAG diagram.

(B) Virus expression indicates GABAergic neurons projections from the vlPAG to the VTA, ZI, and LPO.

(C) Schematic diagram of optogenetic virus injection into the vlPAG and laser implant into VTA (left). Schematic of the EEG recording configuration and righting reflex detection(right).

(D) Immunofluorescence image of optogenetic virus (GFP, green) and fiber.

(E) Optogenetic activation of vlPAG^GABA projections in VTA significantly shortened RORR time (right).

(F) The representative EEG spectrum of the control group (ChR2-group) and the experimental group (ChR2+ group) in 2.0% sevoflurane anesthesia.

(G) Representative EEG spectra of the ChR2-and ChR2+ groups under 1.5% sevoflurane anesthesia.

(H) At 20–22 min of light stimulation under 2.0% sevoflurane anesthesia, the ChR2+ group exhibited a significantly lower BSR of EEG compared to the ChR2-group.

Figure 4. Continued

(I) During 20–22 min of light stimulation under 1.5% anesthesia, the ChR2+ group showed a decrease in the percentage of power in the δ band, along with significant increases in the β and γ bands. Conversely, no significant differences were observed in the ChR2-group.

(J) During 20–22 min of light stimulation under 1.5% sevoflurane anesthesia, the ChR2+ group exhibited a significantly greater body movement score compared to the ChR2-group. The data is presented as the mean $\pm$ SEM, *p < 0.05, **p < 0.01, ***p < 0.001.

During 1.5% sevoflurane maintenance, optical stimulation of ChR2+ mice produced a decrease in delta power (F [2, 15] = 12.87, p = 0.0006), whereas the power in the beta (F [2, 15] = 13.19, p = 0.0005) and the gamma (F [2, 15] = 10.95, p = 0.0012) bands markedly increased (Figure 5K). No difference in EEG power spectra was observed in ChR2-mice after stimulation. Arousal scores in the ChR2+ group were higher than that in the ChR2-group following optical stimulation (Figure 5L).

These results demonstrate that mPFC^{Pyr}-vlPAG projections facilitates arousal from sevoflurane anesthesia.

GABA fluorescent sensor in VTA can follow transients in intact neural circuits

To investigate the existence of third-order mPFC^{Pyr}-vlPAG^{GABA}-VTA projections, we combined optogenetics with fluorescence sensor imaging technology. We injected *rAAV2/9-CamKII-ChrimsonR-mCherry* (120 nL, titter: 2.18 × 10^{12} v.g./mL, unilaterally) into the mPFC and inserted optical fibers into the vlPAG, simultaneously injected *rAAV2/9-hSyn-SF-iGABASnFR.F102G* (150 nL, titter: 4.76 × 10^{12} v.g./mL, unilaterally) and inserted record fibers into the VTA to detect changes in GABA transmitters in the VTA (Figures 6A and 6B).

We used 635 nm red light (10 mW, 20 Hz, 10 ms duration, 1s-on) to stimulate mPFC^{Pyr}-vlPAG projections and recording the release of GABA transmitters in the VTA (Figures 6C and 6D). We found that every second of light stimulation was accompanied by a second increase in the sensor fluorescence signal, indicating the existence of the mPFC^{Pyr}-vlPAG^{GABA}-VTA projection pathway (Figure 6E).

We further investigated the GABA transmitter activities of the VTA *in vivo* across anesthesia-wake states and found that VTA GABA transmitters were suppressed by sevoflurane anesthesia and gradually reactivated as sevoflurane anesthesia faded away (Figures 6F and 6G), implying that VTA GABA release may be involved in regulating sevoflurane anesthesia. The simultaneous recording of fluorescence signal and EEG showed that the EEG signals changed with the elevation of the sensor signal during 2.0% sevoflurane maintenance (Figure 6J), with a decrease in delta power (40.7% $\pm$ 1.3% vs. 24.0% $\pm$ 1.9%, p = 0.0001) and an increase in beta (11.7% $\pm$ 0.7% vs. 18.2% $\pm$ 1.1%, p = 0.0012) and gamma (14.5% $\pm$ 1.3% vs. 20.4% $\pm$ 1.3%, p = 0.0112) bands (Figure 6K), similar to the calcium signals observed in Figure 1.

DISCUSSION

In this study, we used optogenetics, chemogenetics, and fluorescence imaging techniques to confirm the roles of the vlPAG GABAergic neural circuit in regulating arousal during sevoflurane anesthesia. Our findings showed that the activity of GABAergic neurons in vlPAG gradually decreased during anesthesia and increased after recovery from anesthesia, and both optogenetic and chemogenetic activation of vlPAG^{GABA} neurons promoted emergence during the anesthesia maintenance and recovery. Chemogenetic inhibition of vlPAG^{GABA} neurons prolonged emergence from anesthesia, and increased the BSR of EEG during anesthesia. Additionally, we elucidated the role of arousal-promoting vlPAG^{GABA} neurons in the control of the cortico-midbrain pathway. Optogenetic activation of vlPAG^{GABA}-VTA induced the transition from anesthesia state to wakefulness, and that activation of pyramidal neurons in the mPFC-vlPAG circuit accelerated the emergence from general anesthesia and increased the release of GABA neurotransmitter in VTA. These findings demonstrate that the vlPAG nucleus plays a critical role in controlling wakefulness during sevoflurane anesthesia via the cortico-midbrain circuit.

The vlPAG plays a crucial role in regulating REM sleep, as the activation of vlPAG^{GABA} neurons impedes the onset and maintenance of REM sleep. According to Franz Weber et al., the effect of vlPAG^{GABA} neuron activation on the initiation of wakefulness was contingent on the preceding state. Specifically, while the transition from NREM to wakefulness was reduced, the transition from REM to wakefulness was enhanced. Interestingly, the REM-off vlPAG^{GABA} neurons were most active during wakefulness, despite the fact that their optogenetic stimulation increased NREM sleep and decreased wakefulness.[14] While the changes in vlPAG^{GABA} neurons activity during sevoflurane anesthesia may seem inconsistent with its role in promoting
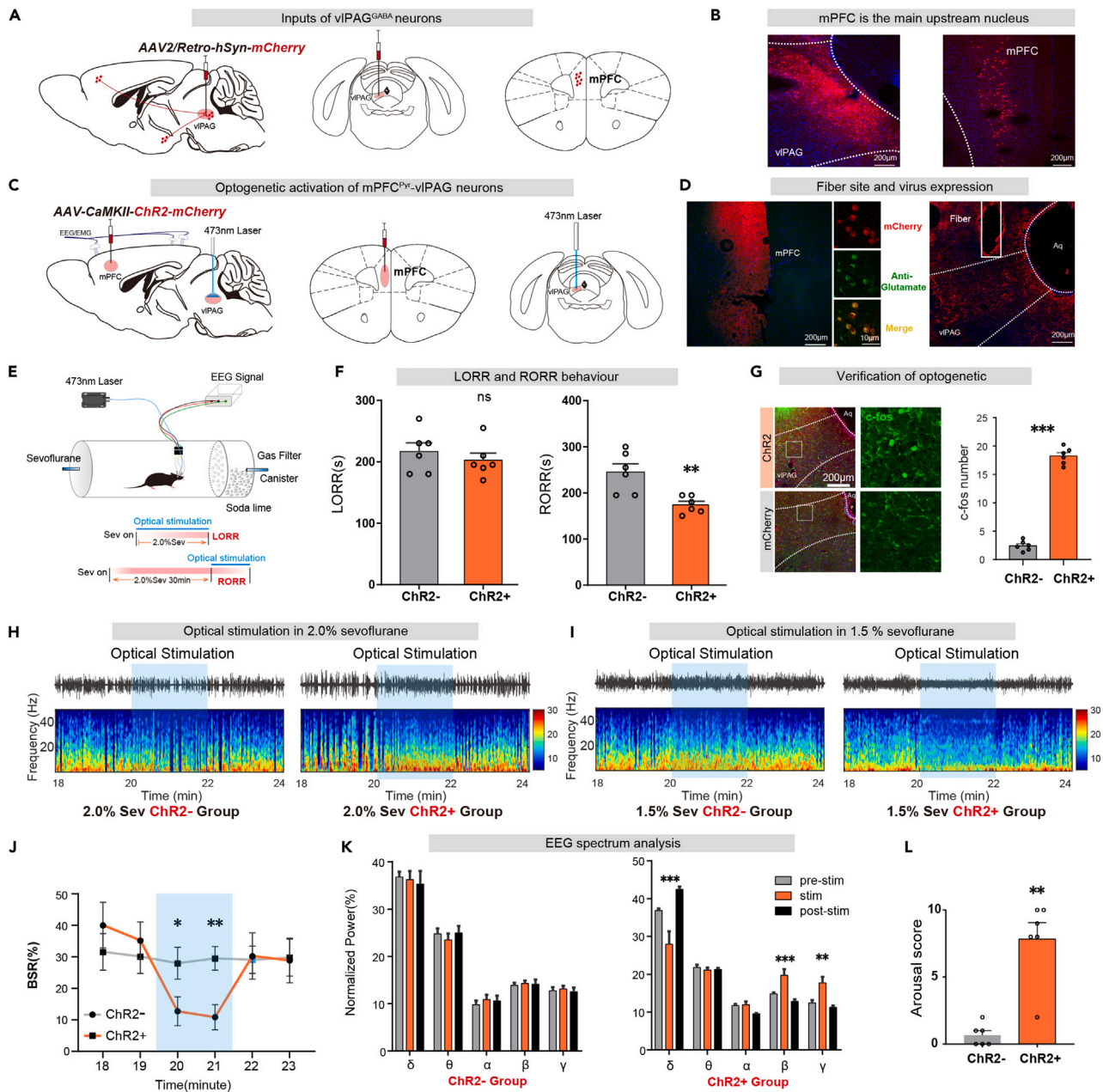
Figure 5. Optical stimulation of mPFC^{Pyr}-vlPAG projections facilitates arousal from sevoflurane anesthesia

(A) Schematic diagram of retrograde tracing by AAV2/Retro virus injection into the vlPAG.

(B) mPFC is an important upstream nucleus.

(C) Injection of optogenetic virus into mPFC and fiber implant into vlPAG, as shown in the schematic.

(D) Immunofluorescence image of optogenetic virus (mCherry, red) expression in mPFC^{Pyr} neurons (Glutamate, green). Virus expression indicates projections from pyramidal neurons in the mPFC to the vlPAG.

(E) EEG recording configuration and righting reflex detection schematic.

(F) Optogenetic activation of mPFC^{Pyr} projections in vlPAG significantly shortened RORR time.

(G) Immunofluorescence of c-fos in vlPAG is increased by optogenetic activation.

(H) The representative EEG spectrum of the ChR2-group and the ChR2+ group under 2.0% sevoflurane anesthesia.

(I) The representative EEG spectrum of the ChR2-group and the ChR2+ group in 1.5% sevoflurane anesthesia.

(J) At 20–22 min of light stimulation under 2.0% sevoflurane anesthesia, the ChR2+ group displayed a significantly lower BSR of EEG compared to the ChR2-group.

Figure 5. *Continued*

(K) During 20–22 min of light stimulation under 1.5% anesthesia, the ChR2+ group exhibited a decrease in the percentage of power in the δ band while the β and γ bands demonstrated a significant increase. Conversely, there was no discernible difference in the EEG spectrum of the ChR2-group.

(L) During 20–22 min of light stimulation under 1.5% sevoflurane anesthesia, the ChR2+ group demonstrated a significantly higher body movement score compared to the ChR2-group. The data is presented as the mean ± SEM, *p < 0.05, **p < 0.01, ***p < 0.001.

NREM sleep, it is important to note that disappearance and recovery of consciousness of anesthesia is a unique state that involves different neural mechanisms compared to sleep.[19] Our findings may prompt further contemplation on the distinctions between anesthesia and REM/NREM sleep. The process of general anesthesia consists of three phases-induction, maintenance, and recovery-are likely mediated by diverse neural pathways, rather than a straightforward mirroring mechanism. Our study revealed that the cortico-midbrain pathway centered on vlPAG^{GABA} neurons plays a significant role in promoting arousal during anesthesia maintenance and recovery, but not during the induction phase of anesthesia.

Descending projections to the PAG primarily originate from the mPFC,[21] which is consistent with our neural tracing results. mPFC-vlPAG projection is involved in aversive and compulsive behavioral responses, as well as pain modulation.[22,23] The PFC is a cortical region thought to modulate consciousness states and is connected reciprocally with wake-promoting brain centers in the brainstem and diencephalon.[20,24,25] Our finding suggested the cortex promote the recovery of sevoflurane anesthesia through a direct descending projection to the midbrain. The PAG sends glutamatergic and GABAergic inputs directly to DA-containing and GABA-containing neurons in the VTA.[26,27] The posterior and ventrolateral segment neurons of PAG are the main projections upstream of VTA, and PAG^{GABA}-VTA afferents are potentially involved in stress, pain, and immobility.[28,29] The VTA comprises a diverse population of glutamatergic and GABAergic neurons in addition to dopaminergic neurons, with VTA^{GABA} neurons activation facilitating general anesthesia, while excitation of VTA^{Glu} and VTA^{DA} neurons promote wakefulness.[30,31] A recent study revealed a specific circuit of GABA-somatostatin neurons in VTA nucleus detects stress and induces restorative sleep.[32] In our supplementary study, we employed light stimulation to activate the vlPAG-VTA GABAergic neurons projections and evaluated changes in c-fos protein expression in VTA via immunofluorescence staining. Our results showed that the expression of c-fos protein decreased in VTA^{GABA} neurons in ChR2+ group. It is suggested that activating vlPAG^{GABA} neurons can inhibit the activity of VTA^{GABA} neurons (Figure S4).

Arousal and anesthesia are believed to be modulated by several excitatory neurotransmitters, including dopamine, noradrenaline, glutamate, and acetylcholine.[33] Meanwhile, GABA, which is the most abundant inhibitory neurotransmitter in the brain, is associated with the initiation and maintenance of sleep through its inhibitory neural circuits.[34] Activation of VTA^{GABA} neurons can significantly deepen anesthesia with isoflurane.[30] GABA in the lateral hypothalamus (LH) projects to the thalamic reticular nucleus (TRN), which promotes isoflurane anesthesia arousal.[35] The regulation of wakefulness and the facilitation of recovery from isoflurane anesthesia are attributed to the involvement of GABAergic neurons in the lateral septum.[36] These findings suggest that inhibitory GABAergic in diverse nuclei can serve discrete functions in inhalation anesthesia. Our investigation enhances the comprehension of the effect of GABAergic neurons in brain nucleus as inhibitory neurons in promoting arousal during the maintenance and recovery periods of anesthesia.

The bottom-up mechanism of anesthesia has been extensively studied in the context of arousal and anesthetic emergence.[37] Prefrontal cortex top-down signals are involved in various neurobiological processes, such as attention, memory, and emotional regulation.[38] Recent studies have demonstrated that cortical neurons can exert powerful top-down control over subcortical domains crucially involved in anesthetic-induced unconsciousness.[4,16] Our study highlights the significant role of the cortico-midbrain pathway in regulating sevoflurane anesthesia.

Overall, our findings demonstrate that GABAergic neurons in the vlPAG are crucial in general anesthesia and that their activation can facilitate arousal from sevoflurane general anesthesia. Our study also reveals the role of tertiary projection mPFC^{Pyr}-vlPAG^{GABA}-VTA centered on GABAergic neurons in the vlPAG during top-down anesthesia arousal. The arousal-promoting effect of GABAergic neurons may offer a new direction to explore the formation and maintenance mechanism of consciousness.

Limitations of the study

Neurons transfected with the GAD67 promoter contain a wide range of GABAergic neurons subtypes, encompassing somatostatin, vasoactive intestinal peptide, and parvalbumin neurons.[39] The specific subtype
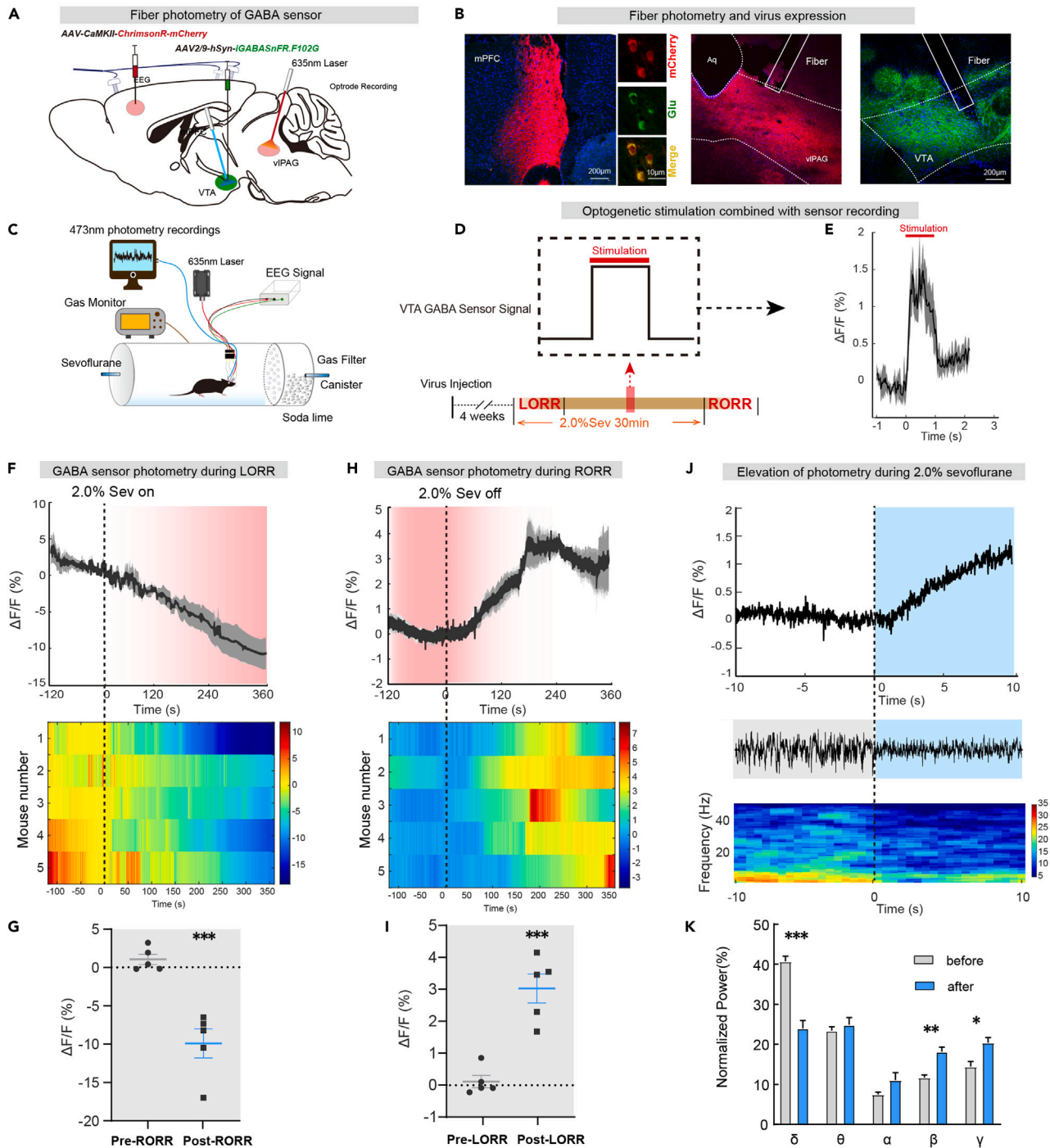
Figure 6. GABA fluorescent sensor in VTA can follow transients in intact neural circuits

(A) Schematic diagram of virus injection.

(B) Virus expression indicates pyramidal neuron projections from the mPFC to the vlPAG and GABA fluorescent sensor expression in VTA.

(C) Schematic of the EEG recording configuration and sensor recording.

(D) Schematic diagram of light stimulation and signal recording mode.

(E) One second of light stimulation was accompanied by a second increase in the sensor fluorescence signal.

(F) After the beginning of 2.0% sevoflurane anesthesia, the activity of GABA sensor signals gradually decreased (top), and the heatmaps changes for five mice (bottom).

(G) The ΔF/F value of GABA sensor signals decreased significantly after the beginning of anesthesia.

Figure 6. Continued

(H) After 2.0% sevoflurane anesthesia, the activity of GABA sensor signals gradually increased (top), and the heatmap changes of five mice (bottom).

(I) The ΔF/F value of GABA sensor signals increased markedly after anesthesia.

(J) Representative elevation changes of GABA sensor signal in VTA and corresponding EEG spectrum during anesthesia.

(K) Trend diagram of the percentage of power in the different frequency bands, related to (J). Data are shown as the mean $\pm$ SEM, $*p < 0.05$, $**p < 0.01$, $***p < 0.001$.

of vlPAG^{GABA} neurons involved in regulating anesthesia arousal remains unclear in our study. Additionally, further research is needed to elucidate the precise connections and roles of the vlPAG^{GABA}-VTA pathway. In future studies, it is crucial to identify the specific targets of vlPAG^{GABA} projections within the VTA.

STAR★METHODS

Detailed methods are provided in the online version of this paper and include the following:

- KEY RESOURCES TABLE
- RESOURCE AVAILABILITY
  - Lead contact
  - Materials availability
  - Data and code availability
- EXPERIMENTAL MODEL AND PARTICIPANT DETAILS
  - Animals
- METHOD DETAILS
  - Virus and drugs
  - Optogenetics
  - Chemogenetics
  - Stereotaxic surgery
  - Coordinates used for the procedures were as follows
  - Fiber photometry
  - EEG recording
  - Behavioral tests
  - Arousal scoring
  - Immunohistochemistry
- QUANTIFICATION AND STATISTICAL ANALYSIS

SUPPLEMENTAL INFORMATION

Supplemental information can be found online at https://doi.org/10.1016/j.isci.2023.107486.

AUTHOR CONTRIBUTIONS

Y.G. performed the experiments, analyzed/interpreted the data, prepared the Figs, and wrote the manuscript. Y.S. performed the experiments, analyzed/interpreted the data, and prepared the Figs. F.C. and Z.Z. performed experiments and analyzed data. W.S. and A.L. revised the manuscript. X.H., J.C., and Y.L. guided the experiment. W.M. and L.T. were responsible for the experiment's conception, design, manuscript writing, and revisions.

DECLARATION OF INTERESTS

The authors declare no competing interests.

REFERENCES

1. Yang, Q., Zhou, F., Li, A., and Dong, H. (2022). Neural substrates for the regulation of sleep and general anesthesia. Curr. Neuropharmacol. 20, 72–84. https://doi.org/10.2174/1570159X19666211214144639.

2. Li, J., Li, H., Wang, D., Guo, Y., Zhang, X., Ran, M., Yang, C., Yang, Q., and Dong, H. (2019). Orexin activated emergence from isoflurane anaesthesia involves excitation of ventral tegmental area dopaminergic neurones in rats. Br. J. Anaesth. 123, 497–505. https://doi.org/10.1016/j.bja.2019.07.005.

3. Ren, S., Wang, Y., Yue, F., Cheng, X., Dang, R., Qiao, Q., Sun, X., Li, X., Jiang, Q., Yao, J., et al. (2018). The paraventricular thalamus is a critical thalamic area for wakefulness. Science 362, 429–434. https://doi.org/10.1126/science.aat2512.

4. Suzuki, M., and Larkum, M.E. (2020). General anesthesia decouples cortical pyramidal neurons. Cell 180, 666–676.e13. https://doi.org/10.1016/j.cell.2020.01.024.

5. Wang, D., Guo, Y., Li, H., Li, J., Ran, M., Guo, J., Yin, L., Zhao, S., Yang, Q., and Dong, H. (2021). Selective optogenetic activation of orexinergic terminals in the basal forebrain and locus coeruleus promotes emergence from isoflurane anaesthesia in rats. Br. J. Anaesth. 126, 279–292. https://doi.org/10.1016/j.bja.2020.09.037.

6. Lacalli, T. (2018). Amphioxus neurocircuits, enhanced arousal, and the origin of vertebrate consciousness. Conscious. Cogn 62, 127–134. https://doi.org/10.1016/j.concog.2018.03.006.

7. Baron, M., and Devor, M. (2022). Might pain be experienced in the brainstem rather than in the cerebral cortex? Behav. Brain Res. 427, 113861. https://doi.org/10.1016/j.bbr.2022.113861.

8. Li, A., Li, R., Ouyang, P., Li, H., Wang, S., Zhang, X., Wang, D., Ran, M., Zhao, G., Yang, Q., et al. (2021). Dorsal raphe serotonergic neurons promote arousal from isoflurane anesthesia. CNS Neurosci. Ther. 27, 941–950. https://doi.org/10.1111/cns.13656.

9. Taylor, N.E., Van Dort, C.J., Kenny, J.D., Pei, J., Guidera, J.A., Vlasov, K.Y., Lee, J.T., Boyden, E.S., Brown, E.N., and Solt, K. (2016). Optogenetic activation of dopamine neurons in the ventral tegmental area induces reanimation from general anesthesia. Proc. Natl. Acad. Sci. USA. 113, 12826–12831. https://doi.org/10.1073/pnas.1614340113.

10. Brown, E.N., Purdon, P.L., and Van Dort, C.J. (2011). General anesthesia and altered states of arousal: a systems neuroscience analysis. Annu. Rev. Neurosci. 34, 601–628. https://doi.org/10.1146/annurev-neuro-060909-153200.

11. Kingsbury, M.A., Kelly, A.M., Schrock, S.E., and Goodson, J.L. (2011). Mammal-like organization of the avian midbrain central gray and a reappraisal of the intercollicular nucleus. PLoS One 6, e20720. https://doi.org/10.1371/journal.pone.0020720.

12. Kittelberger, J.M., Land, B.R., and Bass, A.H. (2006). Midbrain periaqueductal gray and vocal patterning in a teleost fish. J. Neurophysiol. 96, 71–85. https://doi.org/10.1152/jn.00067.2006.

13. Silva, C., and Mcnaughton, N. (2019). Are periaqueductal gray and dorsal raphe the foundation of appetitive and aversive control? A comprehensive review. Prog. Neurobiol. 177, 33–72. https://doi.org/10.1016/j.pneurobio.2019.02.001.

14. Weber, F., Hoang Do, J.P., Chung, S., Beier, K.T., Bikov, M., Saffari Doost, M., and Dan, Y. (2018). Regulation of rem and non-rem sleep by periaqueductal gabaergic neurons. Nat. Commun. 9, 354. https://doi.org/10.1038/s41467-017-02765-w.

15. Zhong, P., Zhang, Z., Barger, Z., Ma, C., Liu, D., Ding, X., and Dan, Y. (2019). Control of non-rem sleep by midbrain neurotensinergic neurons. Neuron 104, 795–809.e6. https://doi.org/10.1016/j.neuron.2019.08.026.

16. Bharioke, A., Munz, M., Brignall, A., Kosche, G., Eizinger, M.F., Ledergerber, N., Hillier, D., Gross-Scherf, B., Conzelmann, K.K., Macé, E., and Roska, B. (2022). General anesthesia globally synchronizes activity selectively in layer 5 cortical pyramidal neurons. Neuron 110, 2024–2040.e10. https://doi.org/10.1016/j.neuron.2022.03.032.

17. Franks, N.P. (2008). General anaesthesia: from molecular targets to neuronal pathways of sleep and arousal. Nat. Rev. Neurosci. 9, 370–386. https://doi.org/10.1038/nrn2372.

18. Minert, A., Baron, M., and Devor, M. (2020). Reduced sensitivity to anesthetic agents upon lesioning the mesopontine tegmental anesthesia area in rats depends on anesthetic type. Anesthesiology 132, 535–550. https://doi.org/10.1097/ALN.0000000000003087.

19. Moody, O.A., Zhang, E.R., Vincent, K.F., Kato, R., Melonakos, E.D., Nehs, C.J., and Solt, K. (2021). The neural circuits underlying general anesthesia and sleep. Anesth. Analg. 132, 1254–1264. https://doi.org/10.1213/ANE.0000000000005361.

20. Zhong, H., Xu, H., Li, X., Xie, R.G., Shi, Y., Wang, Y., Tong, L., Zhu, Q., Han, J., Tao, H., et al. (2023). A role of prefrontal cortico-hypothalamic projections in wake promotion. Cereb. Cortex 33, 3026–3042. https://doi.org/10.1093/cercor/bhac258.

21. Hardy, S.G., and Leichnetz, G.R. (1981). Cortical projections to the periaqueductal gray in the monkey: a retrograde and orthograde horseradish peroxidase study. Neurosci. Lett. 22, 97–101. https://doi.org/10.1016/0304-3940(81)90070-7.

22. Huang, J., Gadotti, V.M., Chen, L., Souza, I.A., Huang, S., Wang, D., Ramakrishnan, C., Deisseroth, K., Zhang, Z., and Zamponi, G.W. (2019). A neuronal circuit for activating descending modulation of neuropathic pain. Nat. Neurosci. 22, 1659–1668. https://doi.org/10.1038/s41593-019-0481-5.

23. Siciliano, C.A., Noamany, H., Chang, C.J., Brown, A.R., Chen, X., Leible, D., Lee, J.J., Wang, J., Vernon, A.N., Vander Weele, C.M., et al. (2019). A cortical-brainstem circuit predicts and governs compulsive alcohol drinking. Science 366, 1008–1012. https://doi.org/10.1126/science.aay1186.

24. Briand, L.A., Gritton, H., Howe, W.M., Young, D.A., and Sarter, M. (2007). Modulators in concert for cognition: modulator interactions in the prefrontal cortex. Prog. Neurobiol. 83, 69–91. https://doi.org/10.1016/j.pneurobio.2007.06.007.

25. Pal, D., Dean, J.G., Liu, T., Li, D., Watson, C.J., Hudetz, A.G., and Mashour, G.A. (2018). Differential role of prefrontal and parietal cortices in controlling level of consciousness. Curr. Biol. 28, 2145–2152.e5. https://doi.org/10.1016/j.cub.2018.05.025.

26. Geisler, S., Derst, C., Veh, R.W., and Zahm, D.S. (2007). Glutamatergic afferents of the ventral tegmental area in the rat. J. Neurosci. 27, 5730–5743. https://doi.org/10.1523/JNEUROSCI.0012-07.2007.

27. Ntamati, N.R., Creed, M., Achargui, R., and Lüscher, C. (2018). Periaqueductal efferents to dopamine and gaba neurons of the vta. PLoS One 13, e0190297. https://doi.org/10.1371/journal.pone.0190297.

28. Kender, R.G., Harte, S.E., Munn, E.M., and Borszcz, G.S. (2008). Affective analgesia following muscarinic activation of the ventral tegmental area in rats. J. Pain 9, 597–605. https://doi.org/10.1016/j.jpain.2008.01.334.

29. Li, C., Sugam, J.A., Lowery-Gionta, E.G., Mcelligott, Z.A., Mccall, N.M., Lopez, A.J., Mcklveen, J.M., Pleil, K.E., and Kash, T.L. (2016). Mu opioid receptor modulation of dopamine neurons in the periaqueductal gray/dorsal raphe: a role in regulation of pain. Neuropsychopharmacology 41, 2122–2132. https://doi.org/10.1038/npp.2016.12.

30. Yin, L., Li, L., Deng, J., Wang, D., Guo, Y., Zhang, X., Li, H., Zhao, S., Zhong, H., and Dong, H. (2019). Optogenetic/chemogenetic activation of gabaergic neurons in the ventral tegmental area facilitates general anesthesia via projections to the lateral hypothalamus in mice. Front. Neural Circuits 13, 73. https://doi.org/10.3389/fncir.2019.00073.

31. Yu, X., Li, W., Ma, Y., Tossell, K., Harris, J.J., Harding, E.C., Ba, W., Miracca, G., Wang, D., Li, L., et al. (2019). Gaba and glutamate neurons in the vta regulate sleep and wakefulness. Nat. Neurosci. 22, 106–119. https://doi.org/10.1038/s41593-018-0288-9.

32. Yu, X., Zhao, G., Wang, D., Wang, S., Li, R., Li, A., Wang, H., Nollet, M., Chun, Y.Y., Zhao, T., et al. (2022). A specific circuit in the midbrain detects stress and induces restorative sleep. Science 377, 63–72. https://doi.org/10.1126/science.abn0853.

33. Kelz, M.B., García, P.S., Mashour, G.A., and Solt, K. (2019). Escape from oblivion: neural mechanisms of emergence from general anesthesia. Anesth. Analg. 128, 726–736.

https://doi.org/10.1213/ANE.
0000000000004006.

34. Mcginty, D., Gong, H., Suntsova, N., Alam, M.N., Methippara, M., Guzman-Marin, R., and Szymusiak, R. (2004). Sleep-promoting functions of the hypothalamic median preoptic nucleus: inhibition of arousal systems. Arch. Ital. Biol. *142*, 501–509.

35. Herrera, C.G., Cadavieco, M.C., Jego, S., Ponomarenko, A., Korotkova, T., and Adamantidis, A. (2016). Hypothalamic feedforward inhibition of thalamocortical network

controls arousal and consciousness. Nat. Neurosci. *19*, 290–298. https://doi.org/10.1038/nn.4209.

36. Wang, D., Guo, Q., Zhou, Y., Xu, Z., Hu, S.W., Kong, X.X., Yu, Y.M., Yang, J.X., Zhang, H., Ding, H.L., and Cao, J.L. (2021). Gabaergic neurons in the dorsal-intermediate lateral septum regulate sleep-wakefulness and anesthesia in mice. Anesthesiology *135*, 463–481. https://doi.org/10.1097/ALN.0000000000003868.

37. Mashour, G.A. (2014). Top-down mechanisms of anesthetic-induced unconsciousness.

Front. Syst. Neurosci. *8*, 115. https://doi.org/10.3389/fnsys.2014.00115.

38. Seth, A.K., and Bayne, T. (2022). Theories of consciousness. Nat. Rev. Neurosci. *23*, 439–452. https://doi.org/10.1038/s41583-022-00587-4.

39. Aime, M., Calcini, N., Borsa, M., Campelo, T., Rusterholz, T., Sattin, A., Fellin, T., and Adamantidis, A. (2022). Paradoxical somatodendritic decoupling supports cortical plasticity during rem sleep. Science *376*, 724–730. https://doi.org/10.1126/science.abk2734.

STAR★METHODS

KEY RESOURCES TABLE

REAGENT or RESOURCE	SOURCE	IDENTIFIER
Antibodies		
Rabbit GABA antibody	GeneTex	CAT#GTX125988; RRID:AB_11173015
Mouse anti-c-fos antibody	Abcam	CAT#ab208942; RRID:AB_2747772
Rabbit anti-Glutamate antibody	Sigma	CAT#G6642; RRID:AB_259946
Alexa Fluor® 488-labelled goat anti-mouse IgG	Servicebio	CAT#GB25301; RRID:AB_2904018
Alexa Fluor® 488-labelled goat anti-rabbit IgG	Servicebio	CAT#GB25303; RRID:AB_2910224
Cy3-labelled donkey anti-mouse IgG	Servicebio	CAT#GB21401
Cy3-labelled donkey anti-rabbit IgG	Servicebio	CAT#GB21403; RRID:AB_2818951
Bacterial and virus strains		
rAAV2/9-GAD67-hM3Dq-mCherry	Obio Biotechnologies	N/A
rAAV2/9-GAD67-hM4Di-mCherry	Obio Biotechnologies	N/A
rAAV2/9-GAD67-mCherry	Obio Biotechnologies	N/A
rAAV2/9-GAD67-hChR2(H134R)-EGFP	Obio Biotechnologies	N/A
rAAV2/9-GAD67-EGFP	Obio Biotechnologies	N/A
rAAV2/9-GAD67-GCaMP6s	Obio Biotechnologies	N/A
rAAV2/9-EF1α-DIO-hChR2(H134R)-EGFP	Obio Biotechnologies	N/A
rAAV2/9-EF1α-DIO-GFP	Obio Biotechnologies	N/A
rAAV2/9-CaMKII-mCherry	Obio Biotechnologies	N/A
rAAV2/9-CaMKII-ChrimsonR-mCherry	Obio Biotechnologies	N/A
rAAV2/9-hSyn-SF-iGABASnFR.F102G	Obio Biotechnologies	N/A
pAAV2/Retro-hSyn-mCherry-2A-Cre	Obio Biotechnologies	N/A
rAAV2/9-DIO-hChR2(H134R)-EGFP	Obio Biotechnologies	N/A
rAAV2/9-DIO-EGFP	Obio Biotechnologies	N/A
rAAV2/9-DIO-mCherry	Obio Biotechnologies	N/A
Chemicals, peptides, and recombinant proteins		
DAPI Fluoromount-G	Southern Biotech	CAT#SBA-0100-20
clozapine-N-oxide	MedChemExpress	CAT#HY-17366
sevoflurane	Baxter Healthcare Corp	CAT#CN2L9117
Normal Donkey Serum	Solarbio	CAT#SL050
Experimental models: Organisms/strains		
Male C57BL/6 mice	Experimental Animal Center of Central South University	N/A
Vgat-ires-Cre mice	the Jackson Laboratory	JAX stock 016962
Software and algorithms		
Prism 8.0	GraphPad	https://www.graphpad.com/
Adobe Illustrator CC 2018	Adobe	https://www.adobe.com/products/illustrator.html
SPSS statistics 25	IBM	www.ibm.com/products/spss-statistics
MATLAB	MathWorks	https://www.mathworks.com/products/matlab

RESOURCE AVAILABILITY

Lead contact

Further information and requests for resources should be directed to and will be fulfilled by the lead contact, tongli301@aliyun.com (Li Tong).

Materials availability

This study did not generate new unique reagents.

Data and code availability

- All data reported in this paper will be shared by the lead contact upon request.
- This paper does not report original code.
- Any additional information required to reanalyse the data reported in this paper is available from the lead contact upon request.

EXPERIMENTAL MODEL AND PARTICIPANT DETAILS

Animals

Animal experiments were conducted using male C57BL/6J mice obtained from the Laboratory Animal Center of the First Medical Center of PLA General Hospital (Beijing, China), and male Vgat-ires-Cre mice provided by Prof. Hailong Dong of Xijing Hospital. Mice were housed in separate cages maintained at 23°C–25°C with 30–50% humidity under a 12/12-h light-dark cycle and had *ad libitum* access to food and water. Ethical approval was obtained from the Ethics Committee for Animal Experimentation of PLA General Hospital, and all animals were 8 weeks old and weighed between 22 and 24 g at the start of the experiment. The animals were randomly numbered and grouped using ear tags. During result assessment, investigators, assessors, raters, and other research personnel were blinded to group assignments. Animals with incorrect virus injection or fiber implantation sites were excluded from the final analysis after behavioral tests. In total, 171 C57BL/6J mice were used, of which 38 lacked expressions in the targeted region or had unexpected expression outside the region, and 11 experienced unexplained deaths. Ultimately, 122 animals were analyzed. The number of animals in each experiment was determined based on previous studies.[2,9]

METHOD DETAILS

Virus and drugs

Unilateral injection of *rAAV2/9-GAD67-EGFP* and *rAAV2/9-GAD67-ChR2-EGFP* viruses was used for optogenetic experiments targeting GABAergic neurons. Unilateral injection of *rAAV2/9-CaMKII-mCherry*, *rAAV2/9-CaMKII-ChR2-mCherry* and *rAAV2/9-CaMKII-ChrimsonR-mCherry* viruses was used for optogenetic experiments targeting pyramidal neurons. Bilateral injection of *rAAV2/9-GAD67-mCherry*, *rAAV2/9-GAD67-hM3Dq-mCherry*, and *rAAV2/9-GAD67-hM4Di-mCherry* viruses were used for chemogenetic experiments, while *rAAV2/9-GAD67-GCaMP6s*, *rAAV2/9-GAD67-EGFP* and *rAAV2/9-hSyn-SF-iGABASnFR.F102G* were constructed for *in vivo* fiber photometry. pAAV2/Retro-hSyn-mCherry-2A-Cre was used for the reverse tracing experiments. All viruses were provided by OBiO Technology Co., Ltd. (Shanghai, China). In addition, immunofluorescence staining was used to verify the specificity of the virus expression. Statistical results showed that about 90% of the neurons expressing fluorescence belonged to GABAergic neurons (Figure S3). Baxter Healthcare Corporation (USA) provided sevoflurane. For chemogenetic experiments, clozapine N-oxide (CNO, 1 mg/kg in saline; MedChemExpress, USA) was administered intraperitoneally before anesthesia.

Optogenetics

Lasers (Thinker Tech, China) delivered light (473 nm and 635 nm) with a power of about 5–10 mW. The mice were subjected to the righting reflex barrel test for 5 min, followed by light stimulation (5-10 mW, 20 Hz, 10 ms duration, 1s-on/1s-off cycle) at the onset of 2.0% sevoflurane anesthesia to measure the LORR time. Three days later, light stimulation was applied at the end of 30 min of 2.0% sevoflurane anesthesia to record the RORR time. EEG and behavioral changes were observed after 2 min of light stimulation during 2.0% and 1.5% anesthesia (20–22 min), respectively. Mice required a 3-day recovery period between each light stimulation experiment.

Chemogenetics

Mice were administered intraperitoneal CNO (1 mg/kg) and, after 1 h, were placed in a righting reflex barrel with EEG electrodes attached. After a 5-min adaptation period, 2.0% sevoflurane anesthesia was administered, and LORR, RORR, and EEG signals were recorded. EEG signals were also recorded under 1.5% sevoflurane anesthesia three days after recovery.

Stereotaxic surgery

Intraperitoneal anesthesia with 2% pentobarbital sodium (40–50 mg/kg) and subscalp anesthesia with 2% lidocaine were administered to mice, which were then secured in a stereotaxic apparatus (RWD, Shenzhen, China) with a heated blanket at 37°C to maintain body temperature. Microinjection pumps (Harvard Apparatus, USA) and 10 μL micro-syringes were used to deliver virus injections at a rate of 40 nL/min, with the syringe remaining stationary for 10 min after injection. Then, electrodes and optical fibers were anchored to the skull using diluted dental cement.

Coordinates used for the procedures were as follows

vlPAG (AP: −4.80 mm, ML: ±0.55 mm, DV: −2.75 mm), VTA (AP: −3.40 mm, ML: −0.60 mm, DV: −4.75 mm), mPFC (AP: +1.98 mm, ML: −0.25 mm, DV: −2.40 mm), LPO (AP: +0.30 mm, ML: −0.6 mm, DV: −5.2 mm), ZI (AP: −1.80 mm, ML: −1.00 mm, DV: −4.5 mm)

For optogenetic and GABA sensor photometry experiments, an optical fiber (diameter: 200 μm, Inper, Hangzhou, China) was implanted into the vlPAG (AP: −4.80 mm, ML: −0.90 mm, DV: −2.85 mm, 10-degree angle to the vertical axis) and a sensor record fiber was implanted into the VTA (AP: −3.30 mm, ML: +0.35 mm, DV: −4.65 mm, 10-degree angle to the vertical axis). A minimum of four weeks was allowed for viral expression before conducting the experiments.

Fiber photometry

Fibre photometry experiments were conducted using a fluorescence photometer fluorescence photometer (Thinker Tech, Nanjing, China) connected to an implanted optical fiber. The light beam was emitted from a 473 nm LED and reflected from a dichromic mirror, and GCaMP6s and GABA sensor (iGABASnFR.F102G) fluorescence were focused and recorded using the photometer. Neurons were activated by a 1-s red laser (635 nm, 10 mW, 20 Hz, 10 ms duration), and changes in sensor signals were observed using the photometer. Laser intensity at the fiber tip was maintained between 40 and 50 μW. Calcium signal intensity was expressed as $\Delta F/F$, where $\Delta F/F = (F_1 - F_0)/F_0 - F_{offset}$. MATLAB (R2020a, MathWorks, USA) was used to analyze changes in $\Delta F/F$.

EEG recording

During anesthesia, the EEG activity of the mice was recorded using the EEG monitor PowerLab and LabChart 8.0 software (ADInstruments, USA) with a sampling frequency of 1000 Hz and band-pass filtering range between 0.3 Hz and 50 Hz. MATLAB (R2020a; MathWorks, Natick, MA, USA) and customized MATLAB codes were used for burst suppression ratio (BSR) and spectral analysis. and customized MATLAB codes. The frequency bands analyzed included delta (δ: 0.3–4 Hz), theta (θ: 4–10 Hz), alpha (α: 10–15 Hz), beta (β: 15–25 Hz), and gamma (γ: 25–50 Hz) waves.

Behavioral tests

Mice were acclimated to a plexiglass cylinder barrel for 5 min prior to the experiment, and the order of measurements was randomized. Sevoflurane concentration was measured using a gas monitor (Datex Engstron, Finland). Anesthesia was induced with 2.0% sevoflurane and 40% O_2 at a flow rate of 2 L/min. The cylinder was rotated 180° every 15 s until the mice experienced a loss of righting reflex (LORR) and lacked the ability to turn prone onto all four limbs. The time period starting from the beginning of sevoflurane inhalation until the LORR occurred was recorded as the induction time. Sevoflurane anesthesia was administered for 30 min and then stopped. After rotating the cylinder as previously described, mice were assessed for how long they were able to independently turn from the supine position with at least three paws touching the bottom. The time elapsed between the cessation of anesthesia and the recovery of righting reflex (RORR) was considered as the emergence time. A heating pad at 37°C was taped to the bottom of the cage throughout the experiment to maintain the mice's body temperature.

Arousal scoring

In the optogenetic experiment, mice were administered 1.5% sevoflurane anesthesia until reaching a stable state. After approximately 20–22 min, light was administered and body movement was assessed according to five previously reported scoring criteria.[5,9] Behavioral scores were summed, up to 10 points per mouse, to calculate the final awakening behavior score. During the experiment, the entire process was video recorded and scored by two researchers in a blinded manner for verification.

Immunohistochemistry

A pentobarbital sodium anesthesia was used to anesthetize mice, which were then transcardially perfused with 0.9% saline followed by 4% paraformaldehyde. Brain slices of 20 μm thickness were obtained using a Leica freezing microtome after dehydration with 20% and 30% sucrose in PBS. The slices were washed thrice with PBS and incubated in 5% donkey serum in PBST (containing 0.3% Triton X-100) for 2 h, followed by incubation with primary antibody in antibody diluent at 4°C overnight. After washing thrice with PBS, the slices were incubated with secondary antibody at room temperature for 2 h in a dim light environment. The brain sections were then washed thrice with PBS, dried, and cover-slipped using DAPI Fluoromount-G (Southern Biotech) before being observed and captured using a fluorescence confocal microscope (Olympus FV1000, Japan). GABA antibody (GeneTex Cat# GTX125988, RRID:AB_11173015, Rabbit, 1:500), anti-*c*-fos antibody (Abcam Cat# ab208942, RRID: AB_2747772, Mouse, 1:1000), anti-glutamate antibody (Sigma-Aldrich Cat# G6642, RRID:AB_259946, Rabbit, 1:1000) were used as primary antibodies, while Alexa Fluor 488 labeled goat anti-mouse, Alexa Fluor 488 labeled goat anti-rabbit, Cy3 labeled donkey anti-mouse IgG, Cy3 labeled donkey anti-rabbit IgG (Servicebio, Wuhan, China) were used as secondary antibodies. We conducted c-fos staining using three animals in each group. Two brain slices per mouse were analyzed by counting the number of c-fos labeled cells within a 500 × 500 μm area of the target nucleus in a blinded manner.

QUANTIFICATION AND STATISTICAL ANALYSIS

We utilized GraphPad Prism 8.0 (GraphPad Software, USA) and SPSS 25.0 Software (IBM, USA) for analysing behavioral and immunofluorescence counting results. We used two-tailed Student's t-tests for comparing two groups, one-way analysis of variance (ANOVA) followed by Bonferroni's multiple comparison test for multiple comparisons, and two-way ANOVA followed by Post Hoc Bonferroni's multiple order for measuring BSR per minute during anesthesia. ANOVA results are expressed as an F-statistic and its associated degrees of freedom and p-value. We adopted the two-tailed Manne Whitney U-test for behavioral scoring during light stimulation. Data were presented as mean $\pm$ SEM, and $p < 0.05$ was considered statistically significant.